

UNCLASSIFIED

AD 4 2 1 6 1 4

DEFENSE DOCUMENTATION CENTER

FOR

SCIENTIFIC AND TECHNICAL INFORMATION

CAMERON STATION, ALEXANDRIA, VIRGINIA



UNCLASSIFIED

NOTICE: When government or other drawings, specifications or other data are used for any purpose other than in connection with a definitely related government procurement operation, the U. S. Government thereby incurs no responsibility, nor any obligation whatsoever; and the fact that the Government may have formulated, furnished, or in any way supplied the said drawings, specifications, or other data is not to be regarded by implication or otherwise as in any manner licensing the holder or any other person or corporation, or conveying any rights or permission to manufacture, use or sell any patented invention that may in any way be related thereto.

CATALOGED BY DDC

AS AD NO. 421614

LIQUID ROCKET PLANT

PRODUCT ENGINEERING PROGRAM

MONTHLY PROGRESS REPORT

on

Coated Metallic Thrust Chambers
Expandable Nozzles
Combustion Instability Scaling Concepts
Ablative Thrust Chambers

Weapon System 107A-2
Contract AF 04(694)-212/SA3

Report 212/SA3-2.2-M-3

15 October 1963



AEROJET-GENERAL CORPORATION

SACRAMENTO, CALIFORNIA

PRODUCT ENGINEERING PROGRAM

Contract AF 04(694)-212/SA3

1 September through 31 September 1963

Prepared by

AEROJET-GENERAL CORPORATION
Liquid Rocket Plant
Sacramento 9, California

Prepared for

BALLISTIC SYSTEMS DIVISION
AIR FORCE SYSTEMS COMMAND
Norton Air Force Base, California

5610



LIQUID ROCKET PLANT SACRAMENTO, CALIFORNIA

A SUBSIDIARY OF THE GENERAL TIRE & RUBBER COMPANY

FOREWORD

This report is the third in a series of monthly reports prepared in accordance with AFBM Exhibit 58-1 and submitted in partial fulfillment of Contract AF O4(694)-212, Supplemental Agreement No. 3.

Direction for contract performance is provided by C. L. D'Ooge, Program Manager, Research and Advanced Technology Division, Liquid Rocket Plant.

The contract for the continuation of the Product Engineering Program is made up of four projects:

	<u>Project Title</u>	<u>Project Engineer</u>
I.	Coated Metallic Thrust Chambers	D. G. Harrington
II.	Expandable Nozzles	D. M. Green
III.	Combustion Instability Scaling Concepts	F. H. Reardon
IV.	Ablative Thrust Chamber Feasibility	T. A. Hughes

The first quarterly review was held at Sacramento on 17 September 1963 with cognizant personnel from USAF Rocket Propulsion Laboratory, Ballistic Systems Division and Aerospace Corporation. The illustrative material used in the presentation has been reproduced and issued on 1 October 1963 as, "Aerojet-General Product Engineering Program, First Quarterly Review."

TABLE OF CONTENTS

	<u>Page No.</u>
I. Coated Metallic Thrust Chambers	I-1
A. Introduction	I-1
B. Progress During Report Period	I-1
C. Next Report Period	I-7
II. Expandable Nozzles	II-1
A. Introduction	II-1
B. Progress During Report Period	II-1
C. Next Report Period	II-6
III. Combustion Instability Scaling Concepts	III-1
A. Introduction	III-1
B. Progress During Report Period	III-2
C. Next Report Period	III-7
Appendix III-A	III-A-1
IV. Ablative Thrust Chambers	IV-1
A. Introduction	IV-1
B. Progress During Report Period	IV-1
C. Next Report Period	IV-3
V. Program Reporting	V-1

TABLE LIST

	<u>Table No.</u>
Performance Parameters	I-1
Thermal Shock Test Results	I-2
Coated Metallic Chamber Milepost Chart	I-3
Expandable Nozzle Milepost Chart	II-1
Combustion Instability Scaling Concepts Milepost Chart	III-1
Ablative Thrust Chambers Feasibility Milepost Chart	IV-1
Program Reporting Milepost Chart	V-1

FIGURE LIST

	<u>Figure No.</u>
Skirt Area After Third Firing of Chamber 1	I-1
Throat Section After Third Firing of Chamber 1	I-2
Divergent Section After Third Firing of Chamber 1	I-3
Chamber Sections and Flange After Third Firing of Chamber 1	I-4
Variable Length TCA	III-1
Preliminary Test Schedule	III-2
Hydraulic - Electric System for Combustion Chamber Elongation	III-3

I. COATED METALLIC THRUST CHAMBERS

A. INTRODUCTION

1. Purpose

The objective of this project is to develop a reliable thermal barrier capable of surface temperature operation above 3300°F for use on regeneratively-cooled thrust chambers employing N_2O_4 /AeroZINE 50 propellants. Thermal barrier coatings are used for improving liquid rocket engine performance through reductions in film-cooling requirements.

2. Approaches

The development of the thermal barriers will be accomplished through:

- a. Full-scale testing of coated YLR91-AJ-5 thrust chambers (Titan II second stage) at fuel-film-cooling flow of 5% or less.
- b. Laboratory thermal shock, thermal conductivity, erosion-corrosion, and metallographic testing.

B. PROGRESS DURING REPORT PERIOD

1. Full-Scale Testing

The first coated combustion chamber, S/N 111, was test fired for the third time on 6 September 1963. The film-cooling was reduced from 17.6 to 5% and the duration was the planned 5 sec. The major test parameters for the three tests to date are listed in Table I-1. The gain of 4.7 lb-sec/lb in specific impulse in the third test was attributed to the reduced film-cooling.

The coating overlay damage which occurred in the first two tests was discussed in the July progress report.⁽¹⁾ In the third test, further flaking

(1) Report 212/SA3-2.2-M-2, 15 August 1963

I, B, Progress During Report Period (cont.)

of the zirconia overlay occurred above and below the throat. However, the three base layers of the coating remained intact over the entire coated surface of the chamber tubes.

The thermal resistance of the three base layers was approximately $160 \text{ in.}^2\text{-sec-}^\circ\text{F/Btu}$, which is calculated to be capable of reducing the heat flux by about 35% in the throat at 5% fuel-film-cooling. The corresponding burnout heat flux ratio is reduced from 1.0 to 0.65. The heat flux ratio is 0.8 for design burnout. The appearances of the coating after the third test in the skirt section, throat, divergent section and chamber section are shown in Figures I-1, I-2, I-3 and I-4, respectively. In the throat the overlay had flaked over a larger area than before, but the three base layers remained and no burnouts occurred. The melting that is visible in Figure I-2 is probably Nichrome which has a melting point of 2500°F . The source was primarily from a 0.054-in. thick coating that was applied to the flange cover plate at the injector interface and secondarily from the third layer of the coating. The calculated operating temperature of the coating surface is 2800°F after the overlay has flaked off.

In the chamber section, flaking of the zirconia overlay occurred on the tube crowns in the third test only. This indicates that the flaking is primarily a function of heat flux and temperature, since this area did not flake in two tests at 17.6% fuel-film-cooling. Vibration apparently was not a major factor.

Three pinhole burnouts occurred in the chamber section tubing, all within 3 inches of the flange cover plate. The failure pattern indicated

I, B, Progress During Report Period (cont.)

that several areas close to the injector were heated much more severely than others. There was also erosion of the 17th channel of the injector. The fact that there were several wide areas with no erosion indicates that the design was close to being effective with the reduced film cooling. The design of a replacement injector is discussed later in this section.

Bulk rise in the fuel coolant was measured with three miniature thermocouple probes, two in the injector feed slots and one in the up-tube manifold. The average bulk rise was 131°F. A calculation of bulk rise was made using the exact conditions of test pressure, mixture ratio, and flow rates established in the third test. The results were about 10°F higher than previously predicted⁽¹⁾ with nominal test conditions. The new calculations predict a rise of 122°F when a thermal resistance of 160 in.²-sec-°F/Btu and film cooling of 5% is assumed. One explanation for the higher bulk rise could be that the effective film cooling was less than 5% because the thick coating on the flange cover plate tended to disrupt the flow. For instance with a thermal resistance of 160 in.²-sec-°F/Btu, 2% film cooling should produce a bulk rise of 131°F.

2. Design

To minimize the erosion of the 17th channel, a design study has been made to improve the 5% film-cooling injector. The following changes are to be made:

(1) BSD-TDR-119, "Development of Thermal Barrier Coatings for Regeneratively-Cooled Rocket Engine Thrust Chambers," 28 June 1963, Figure 21, Appendix A

I, B, Progress During Report Period (cont.)

a. Increase thickness of the 17th channel ring in the area of the injector flange face which will decrease the inside diameter of the 17th channel wall to 0.040-inch smaller than the inside diameter of the coated section face of the combustion chamber. This will minimize the tendency to under-cut the combustion chamber flange coating and also will provide better film cooling of the combustion chamber flange.

b. "Swirl" the film cooling orifices 20° to 30° as on the Apollo service module engine injector i.e., angle the film-cooling distribution on the surface of 17th channel.

c. Impinge the film-cooling spray higher on the 17th channel wall. This will increase the effectiveness of the flange cooling.

d. Tighten the film cooling orifice location tolerances. Make a jig that will allow the orifices to be made so that the height of the impingement point does not vary more than ± 0.010 inch.

e. Increase the active fuel flow in the 17th channel. This will give a lower mixture ratio and will minimize the erosion in the area of the injector flange.

f. Angle the 17th channel actives inward 20° to 30° . Presently, the orifices are angled 40° toward the center of injector. This should lower the temperature in the area of the injector 17th channel.

The above changes will not affect the percent film-cooling. Incorporation of these modifications on the present 2SIN-0-type injector appears

I, B, Progress During Report Period (cont.)

to be the most effective solution to the flange erosion problem experienced with Injector 1022 on the firing of 6 September 1963.

3. Fabrication

Chamber 2, (S/N 085) is complete and has been delivered to the laboratory for coating. Chamber 3 is on schedule for completion 9 October 1963. Chamber 4 will be either Chamber 1, 2, or 3 recoated. Chamber 5 will be coated on 17 March 1964.

The modifications for the chamber coating fixture are progressing well. The fixture was partially modified in order to coat Chamber 2 on schedule; however, the time required to obtain a 5% film-cooling injector to use in testing the chamber resulted in the decision to complete the modifications to the fixture before the coating operation. Subsequently it was decided to initiate testing of Chamber 2 using an available 17.6% fuel-film-cooled injector, but it was too late to withhold the final modifications of the fixture. Consequently, it appears that Chamber 2 will be coated and tested four to six weeks behind schedule. Testing of Chamber 2 with 17.6% fuel-film cooling will be completed early in November.

It should be possible to coat and test Chamber 3 on schedule, providing a timely selection of the coating is made. The testing is scheduled to begin 21 November and the new 5% fuel-film-cooling injector is scheduled for completion 25 November.

I, B, Progress During Report Period (cont.)

4. Laboratory Testing

Sixteen thermal shock specimens were prepared and tested. The results of these tests are shown in Table I-2. The topcoat, or overlay, was considered to be the principle variable since the graded Nichrome-zirconia base coats had performed successfully on Chamber 1. The overlays tested were mixtures of 10, 25, and 50% by weight tungsten in both zirconia and thoria: zirconia, applied in a single pass and in four passes; and a non-graded coating of 50% by weight tungsten and 50% by weight thoria. The thicknesses to be applied were each adjusted for thermal conductivity, so that the total thermal resistance of each specimen would be similar. Each specimen was tested two or three times using either a standard nitrogen-hydrogen plasma gas (highly oxidizing in these open air tests) or a gas mixture of simulated combustion products in which methane and oxygen are added to the plasma gas downstream of the arc. The pure zirconia overlays flaked in two cycles (20 seconds duration each) as before on the previous contract⁽¹⁾ in the standard test. There was no difference between coatings applied with a pass of 0.004-inch or with four passes of 0.001-inch each. In the combustion gas simulation test, the heat flux was more uniform, covered a larger area, and was slightly less; consequently, the pure zirconia overlays were unaffected in 20 cycles of 20 seconds under these conditions. All the tungsten-bearing coatings oxidized rapidly in the standard test atmosphere. In the simulated combustion gas atmosphere, the 10% tungsten

(1) AF 04(647)-652/SA4

I, B, Progress During Report Period (cont.)

coatings showed less oxidation than the 25 and 50% tungsten coatings and generally survived 20 cycles without much damage. Thoria appears to be superior to zirconia in the tungsten mixtures, although further testing will be required to determine definitely which is the better.

Unfortunately, the test series was inconclusive in that no obvious improvement to the overlay was found by the addition of tungsten. The flaking problem does appear to be less with the tungsten present, but oxidation on the outside becomes a problem. At this point it appears that the oxidation rate will have to be determined in a full-scale test; Chamber 2 will be coated accordingly with gradated Nichrome-zirconia with an overlay of 5 mils of 10% by weight tungsten in zirconia.

5. Quality Control Studies

A contract was negotiated with Pyrco Division of Anamet Laboratories for a coating thickness measurement study. The work is progressing well and it appears from experimental results so far on flat and tubular specimens that the eddy current method using a Durmatron unit is the best approach. Calibrations showed much better accuracy on gradated Nichrome-zirconia systems than anticipated. A final report on this work is due 11 October 1963. A follow-on contract is being considered which will include delivery of the eddy current equipment and calibration data to Aerojet-General.

C. NEXT REPORT PERIOD

The coating fixture modifications, including a dust collection system, will be completed and the equipment installed. Chamber 2 will be coated with

I, C, Next Report Period (cont.)

gradated Nichrome-zirconia base, and probably 10% by weight tungsten-zirconia as the overlay.

Additional thermal shock specimens will be prepared and tested to determine the coating selection for Chambers 2 and 3.

The design drawings for a 5% fuel-film-cooling injector will be completed and modifications begun on an existing injector.

Table I-1 is the schedule of tasks for the coated metallic thrust chambers program.

TABLE I-1

PERFORMANCE PARAMETERS

	Test Number		
	<u>1.2-05-RLM-401</u>	<u>1.2-05-RLM-402</u>	<u>1.2-05-RLM-403</u>
Date	7-16-63	7-18-63	9-6-63
Duration, sec	12.6	12.5	5.28
P _{oJ} , psig	982.2	994.7	991.2
P _{fJ} , psig	966.7	977.5	1035
P _c , psia	823.7	832.4	845.3
T _{oJ} , °F	70.57	69.03	81.57
T _{fJ} , °F	147.8	140.6	218, 212, 217
T _{ci} , °F	69.52	66.42	85
F(SL), lb	73,899	74,732	76,900
W _o , lb/sec	202.48	205.05	211.03
W _f , lb/sec	108.15	108.83	105.86
I _s (SL), sec	237.9	238.1	242.7
M.R.	1.872	1.884	1.993
FFC, %	17.6	17.6	5

DEFINITION OF PARAMETERS

P _{oJ}	Injector Oxidizer Pressure
P _{fJ}	Injector Fuel Pressure
P _c	Combustion Chamber Pressure
T _{oJ}	Injector Oxidizer Temperature
T _{fJ}	Injector Fuel Temperature
T _{ci}	Fuel Temperature at Chamber Inlet
F(SL)	Thrust (Sea Level)
W _o	Oxidizer Flow Rate
W _f	Fuel Flow Rate
I _s (SL)	Specific Impulse (Sea Level)
M.R.	Mixture Ratio
FFC	Fuel Film Cooling to Combustion Chamber

TABLE I-2
THERMAL SHOCK TEST RESULTS
TOPCOAT EVALUATION

Specimen No.	Topcoat(1)	Simulated Exhaust Conditions 61 ft ³ /hr CH ₄ 112 ft ³ /hr O ₂ or Air	Heat Flux BTU in ² sec	Cycle Length (sec)	Number Cycles to Damage	Total Cycles	Calculated Thermal Resistance in ² sec-°F in.	Calculated Surface Temperature (°F)	Comparative Appearance After Test(2)	
									Failure Type	Primary Secondary
123	ZrO ₂ ZrO ₂	Exh. Air	6.6 7.3	20 20	10 7	20 12	317 317	3300 3620	A Sintered C	Melt 2
124	10W+90ZrO ₂	Exh. Air	6.6 7.3	20 20	10 2	20 2	284 284	3090 3370	A Sintered D Slight	Melt 2
116		Exh. Exh. Air Exh.	6.6 6.6 7.3 6.6	20 20 20 20	5 2 1 10	6 20 2 20	370 370 370 354	3660 3660 4000 3550	Flake A Chem.Reac. Flake A Spall C A Sintered	Same Chem. Reac.
125		Air	7.3	20	1	1	354	3900	Flake B Chem.Reac.	Melt 1
126		Exh. Air	6.6 7.3	20 20	10 3	20 20	320 320	3330 3640	A C	Sintered Melt 2
121	10W+90ThO ₂	Exh. Exh. Air	6.6 6.6 7.3	20 20 20	3 10 2	20 20 4	282 282 282	3080 3080 3360	A A B	Sintered Sintered
117	25W+75ZrO ₂	Exh. Exh. Air	6.6 6.6 7.3	20 20 20	5 14 2	6 20 2	344 344 344	3490 3490 3820	A A F	Sintered Sintered
122		Exh. Exh. Air	6.6 6.6 7.3	20 20 20	4 10 3	20 20 4	304 304 304	3220 3220 3520	Flake A Flake A Melt 2 C	Sintered Sintered
127		Exh. Air	6.6 7.3	20 20	7 2	13 2	366 366	3640 3970	Flake B F	Sintered Melt 1 Melt 2

TABLE I-2 (cont.)

Specimen No.	Topcoat (1)	Simulated Exhaust Conditions 61 ft ³ /hr CH ₄ 112 ft ³ /hr O ₂ or Air	Heat Flux BTU in ² sec (sec)	Cycle Length (sec)	Number Cycles to Damage	Total Cycles	Calculated Thermal Resistance in ² sec-°F in.	Calculated Surface Temperature (°F)	Comparative Appearance After Test (2)	
									Failure Type	Primary Secondary
128	25W+75ZrO ₂	Exh.	6.6	20	1	2	382	3750	C	Sintered
		Air	7.3	20	3	17	382	4080	C	Melt 2
120	25W+75ThO ₂	Exh.	6.6	20	3	5	273	3020	B	Melt 2
		Exh.	6.6	20	2	7	273	3020	C	Melt 2
118	50W+50ZrO ₂	Air	7.3	20	2	3	273	3300	B	Sintered
		Exh.	6.6	20	1	5	289	3130	D	Glazed
		Exh.	6.6	20	1	2	289	3130	D	Melt 2
		Air	7.3	20	2	4	289	3420	D	Melt 2
129		Exh.	6.6	20	9	11	294	3160	Flake	D Chem.Reac. Melt 3
		Air	7.3	20	2	5	294	3440	D	Melt 3
130		Exh.	6.6	20	3	11	301	3210	D	Glazed
		Air	7.3	20	2	5	301	3500	D	Melt 3
112	50W+50ThO ₂ * 50W+50ThO ₂	Exh.	6.6	20	16	16	239	2800	A	Sintered
		Exh.	6.6	20	2	20	239	2800	A	Small Chem.Reac.
		Air	7.3	20	8	10	239	3050	Melt	C Chem.Reac.
119		Exh.	6.6	20	1	20	300	3200	Flake	D Sintered
		Exh.	6.6	20	5	18	300	3200	Flake	B Melt 1
		Air	7.3	20	2	3	300	3490	Melt	3 D

TABLE I-2 (cont.)

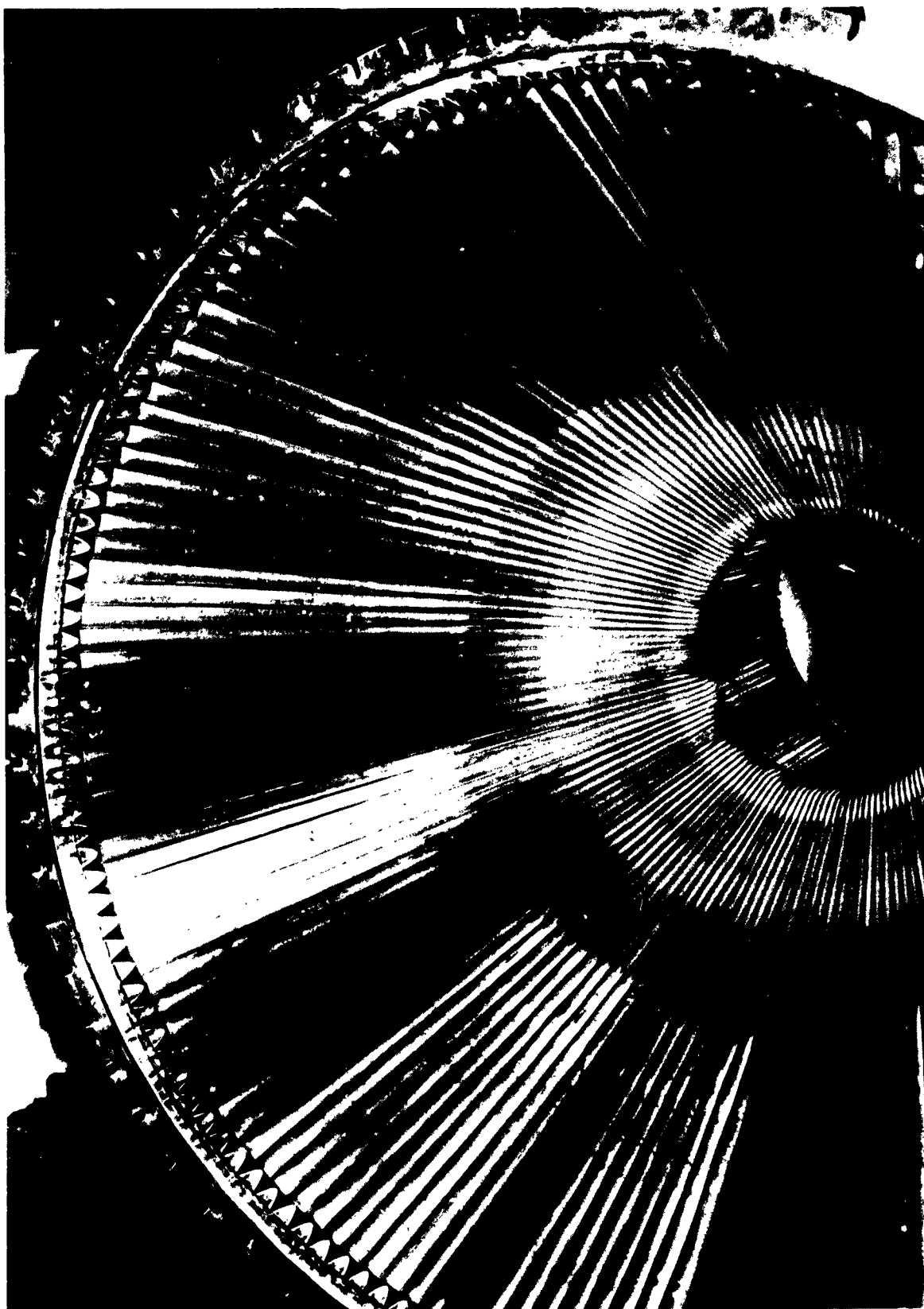
Specimen No.	Topcoat (1)	Simulated Exhaust Conditions 61 ft ³ /hr CH ⁴ 112 ft ³ /hr O ₂ or Air	Heat Flux Btu in ² sec	Cycle Length (sec)	Number Cycles to Damage	Total Cycles	Calculated Thermal Resistance in ² sec-°F in.	Calculated Surface Temperature (°F)	Comparative Appearance After Test(2)
(1)	Base Coat								
	4 mil NiCr								
	4 mil 70 NiCr + 30 ZnO ₂			147	in ² -sec. °F Btu				
	4 mil 50 NiCr + 50 ZnO ₂								
	Test Coat			123	in ² -sec. °F Btu				
	Total Thermal Resistance			270	in ² -sec. °F Btu				
(2)	Failure								Appearance
	Spall								Sintered
	Flake								Glazed
	Melt								Melt
									1 - Selective
									2 - Globular
									3 - Ran
									Chemical Reaction
									1 - Slight
									2 - Medium
									3 - Advanced

* Non-Graded

TABLE I-3 (cont.)

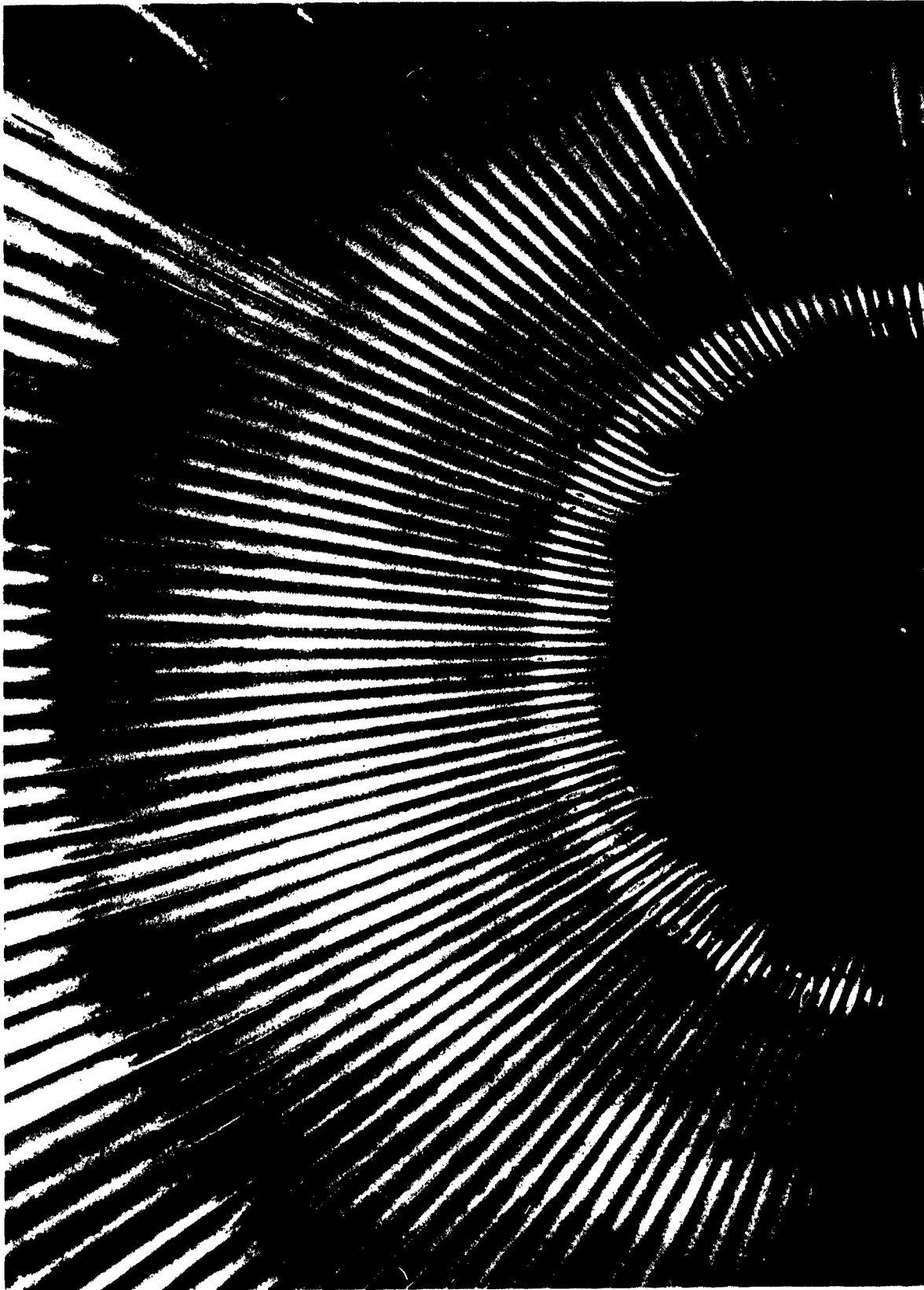
COATED METALLIC THRUST CHAMBERS	PRESENT SCHEDULE			R I P	CY 63					CY 64					
	DAY	MO	YR		J	J	A	S	O	N	D	J	F	M	A
PHASE IV, FULL SCALE TESTING															
A. Thrust Chamber 1															
1. Ready for Buildup	1	6	63	A											
2. Ready for Testing	7	7	63		A										
3. Testing Completed	6	9	63				A								
B. Thrust Chamber 2															
1. Release for Fabrication	1	6	63	A											
2. Ready for Coating	5	9	63				A								
3. Ready for Buildup	20	10	63				◊		▲						
4. Ready for Testing	30	10	63				◊		▲						
5. Testing Completed	15	11	63				◊		▲						
C. Thrust Chamber 3															
1. Release for Fabrication	1	6	63	A											
2. Ready for Coating	9	10	63						▲						
3. Ready for Buildup	23	10	63						▲						
4. Ready for Testing	21	11	63						▲						
5. Testing Completed	8	12	63						▲						
D. Thrust Chamber 4															
1. Remove Previous Coating	1	12	63						▲						
2. Ready for Coating	23	12	63						▲						
3. Ready for Buildup	9	1	64						▲						
4. Ready for Testing	13	2	64						▲						
5. Testing Completed	29	2	64						▲						
E. Thrust Chamber 5															
1. Release for Fabrication	1	9	63												
2. Ready for Coating	17	3	64											▲	
3. Ready for Buildup	2	4	64											▲	
4. Ready for Testing	30	4	64											▲	
5. Testing Completed	30	5	64											▲	
F. Injector 1															
1. Release for Modification	25	7	63		A										
2. Ready for TCA Buildup	3	9	63				A								
G. Injector 2															
1. Release for Fabrication	15	10	63						▲						
2. Ready for TCA Buildup	25	11	63						▲						

◊ - PRESENT SCHEDULE DATE ▲ - ACCOMPLISHED
 P - POTENTIAL CHANGE IN SCHEDULE ◊ - PREVIOUS SCHEDULE DATE



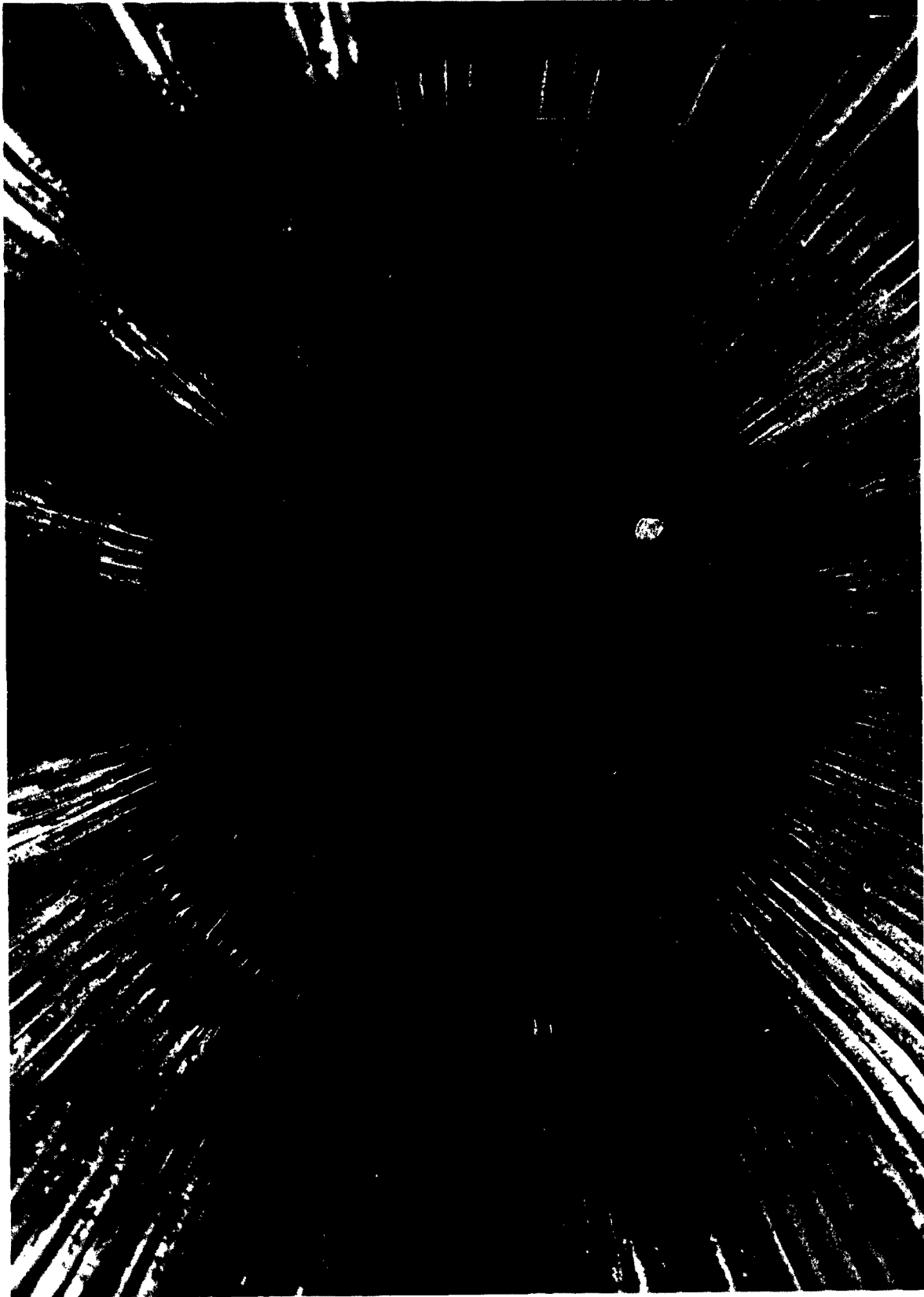
Skirt Area After Third Firing of Chamber 1

Figure I-1



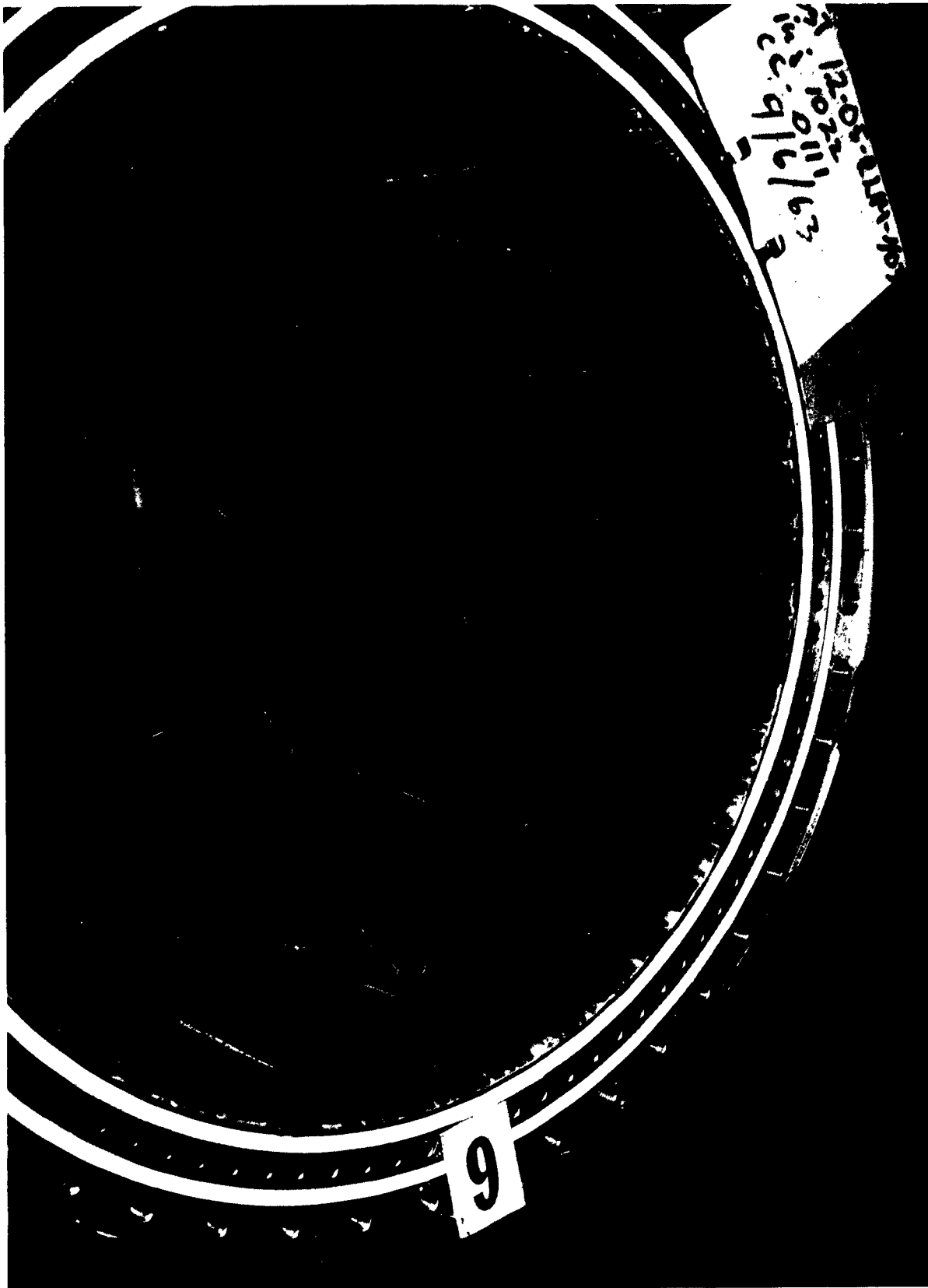
Throat Section After Third Firing of Chamber 1

Figure I-2



Divergent Section After Third Firing of Chamber 1

Figure I-3



Chamber Sections and Flange After Third Firing of Chamber 1

Figure I-4

II. EXPANDABLE NOZZLES

A. INTRODUCTION

1. Purpose

The purpose of this project is to develop and test high expansion ratio expandable nozzle cones for rocket propulsion systems.

2. Approach

The program objectives will be accomplished by a three-phase (design, fabrication and experimental) effort. Work will be directed to simulate the operational nozzle conditions of the Titan II second stage engine with both metallic and non-metallic nozzle expansion cone skirt extensions. Thrust vectoring and internal gas dynamic conditions will be investigated utilizing a bi-propellant liquid rocket engine (12,000-lb thrust) mounted on a multi-axis thrust stand. A series of flight simulation tests in a wind tunnel will be conducted with scale models using various forebody shapes.

B. PROGRESS DURING REPORT PERIOD

1. Theoretical and Design Engineering

For the theoretical analysis of heat transfer, corrections have been made to the computer program which is used to predict radiation equilibrium temperatures of metal skirts. These corrections are to adjust for combustion temperature losses that cause decreased performance (notably losses in characteristic velocity). The exactness of the corrections is being examined to determine whether a better correlation of calculated radiation temperatures and measured temperatures can be obtained. To consider the losses resulting from combustion inefficiency, the difference was adjusted in the temperatures by the following equation:

II, B, Progress During Report Period (cont.)

$$T_{\text{combustion effective}} = \left(\frac{c^* \text{ measured}}{c^* \text{ calculated}} \right)^2 T_{\text{combustion calculated}}$$

Here it is assumed that the properties of the nozzle gas stream, such as γ and molecular weight, are not affected by the injector combustion losses; also that losses in combustion are reflected only in the stagnation temperature of the rocket gases.

In the area of theoretical structural studies, a simplified analysis has been made on the corrugated metal expandable nozzle for use in design calculations. A description of the problem, assumptions, and conclusions is given below:

Problem: It is desired to determine the critical buckling load of a corrugated frustum having a graduated axial load with a free end at the exit and a constrained end at the attachment point.

Assumptions:

- (a) The corrugations will be treated individually as columns having one free end and one attached end. The individual effects of the columns will then be grouped together to simulate the corrugated cone.
- (b) The axial load is assumed to vary parabolically along the axial length of the nozzle. A plot of the thrust with length shows this is very nearly true.
- (c) The cross sectional moment of inertia of the column is assumed to vary in the same manner axially as the load (ie., parabolically).
- (d) The only loads on the columns will be the axial loads and this is resisted by the stiffness of the structural material.

II, B, Progress During Report Period (cont.)

(e) The elastic modulus (E) will be taken at the elevated temperature predicted by the radiation heat transfer computer program.

Conclusions:

(a) The problem is analyzed mathematically by use of the following differential equation:

$$EI_2 \left(\frac{x}{l}\right)^n \frac{d^2y}{dx^2} = q_2 \left(\frac{x}{l}\right)^p y$$

Where

x = distance from the free end

q_2 = thrust load at attachment point of the flexible nozzle

I_2 = the section moment of inertia at the attachment point of the nozzle

Both "n" and "p" are given values of 2.

(b) The critical buckling load is given as:

$$P_{cr} = m \frac{EI_2}{l^2} \text{ where } m = 18.9 \text{ for } n = 2, p = 2$$

(c) If corrugations are assumed to be similar to the ones used on previous nozzles, ⁽¹⁾ the moment of inertia of the corrugated structure around its own centerline is given as:

$$I_2 = \pi Dh^2t - \frac{4}{3} h^3tN \sqrt{\frac{1 + m^2}{m^2}}$$

Where

D = Diameter at attachment point

h = Height of corrugation

m = Geometric factor for corrugation in expanded condition. $m \approx 0.5$

(1) AF O4(647)-652, SA33

II, B, Progress During Report Period (cont.)

N = Number of corrugations

t = Thickness of wall at attachment point

(d) By checking the above formula with the last nozzle geometry tested in the Tullahoma series of 1962-63,⁽¹⁾ the critical load is

$$P_{cr} = 1530 \text{ lb for } E = 30 \times 10^6 \text{ or } 780 \text{ lb for } E = 15 \times 10^6$$

The thrust load developed was 1200 lb due to the effect of the expandable skirt. Since the skirt did not buckle, the above analysis gives conservative estimates of critical buckling load.

(e) Application of the above formula to the Lark size expandable nozzle gives critical buckling loads of 315 lb which is approximately double the thrust of the entire engine. This conservative margin on the small scale is desirable, because the column analysis and assumptions may not be as valid for small size models.

(f) When the equation is applied to the full-scale nozzles to be tested in the J-4 tunnel at AEDC during the current contract, the critical load is predicted to be approximately 6000 lb which is greater than the expected thrust load resulting from the expandable skirt.

Design efforts for the experimental test hardware are progressing on schedule without any major problem areas.

2. Fabrication

Three experimental Lark nozzles with the pressure tube deployment and stabilization concept were completed and demonstrated. Data obtained

(1) AF 04(647)-652, SA33

II, B, Progress During Report Period (cont.)

from the fabrication of these three nozzles will be used in the fabrication of four to six prototype models of the Titan nozzles for tests on the 12K engine.

Three each of 13 nozzles for the 12K thrust vector control phase have been delivered, along with one throat section, to the Azusa Proving Grounds for testing.

Bids have been received for the Titan-size rubber nozzles and work will be initiated during October 1963.

Fabrication was started on the wind tunnel models and various supporting hardware.

3. Testing

No Lark tests were conducted during this report period, but they will be resumed immediately.

Three checkout firings were made on the 12K TVC test phase. Each of the first two firings was of one-second duration with satisfactory test stand operation. The third test was for a duration of three seconds, during which severe engine hardware damage was sustained. Examination of the hardware and recorded data (tape, oscillograph, and motion pictures) indicated the origin and type of failure. There was erosion of the chamber near the injector in a scalloped pattern. The number of scallops corresponded to the number of injector elements in the outer ring. This scalloping effect on the periphery of the injector face, coupled with an inferior gasket seal between the injector and chamber, led to a hot-gas leak. The hot-gas leak increased the erosion and caused a burn-through to the oxidizer manifold. The spraying of high pressure oxidizer

II, B, Progress During Report Period (cont.)

on the walls and throat caused severe damage to the chamber wall and throat insert. The injector and throat insert were lost but the chamber was repaired.

A backup injector and throat insert will be installed and testing resumed. A gasket seal change was also made. The backup injector is a copper-faced model and the outer injector pattern has been redrilled to spray axially along the chamber wall.

No other testing was conducted during this report period.

C. NEXT REPORT PERIOD

All hardware and nozzle design work will be completed.

Lark nozzle fabrication will be continued. Fabrication of the Titan-size nozzles and component hardware will be initiated.

Lark and 12K TVC testing will be resumed.

Table II-1 presents the schedules of tasks for the expandable nozzle program.

Table II-1
Expandable Nozzle Milepost Chart

EXPANDABLE NOZZLES	PRESENT SCHEDULE			R	CY 63												CY 64											
	DAY	MO	YR		J	J	A	S	O	N	D	J	F	M	A	M												
PHASE I, ENGINEERING DESIGN																												
A. Refinement and Correlation of Design Progress																												
1. Initiated	1	6	63	A																								
2. Completed	31	5	64															▲										
B. Lark Test Hardware																												
1. Initiated	1	6	63	A																								
2. Completed	31	8	63				A																					
C. 12K Test Hardware																												
1. Initiated	1	6	63	A																								
2. Completed	31	9	63																									
D. Titan Size Hardware																												
1. Initiated	1	7	63	A																								
2. Completed	30	11	63								▲																	
E. Wind Tunnel Flight Simulation Test Hardware																												
1. Initiated	1	8	63	A																								
2. Completed	28	2	64															▲										
PHASE II, FABRICATION																												
A. Lark Hardware																												
1. Initiated	1	7	63	A																								
2. Completed	31	12	63																									
B. 12K Hardware																												
1. Initiated	1	7	63	A																								
2. Completed	31	12	63																									
C. Titan Size Hardware																												
1. Initiated	1	9	63	A																								
2. Completed	28	2	64															▲										
D. Wind Tunnel Support and Misc. Hardware																												
1. Initiated	1	9	63	A																								
2. Completed	28	2	64															▲										
E. Wind Tunnel Vehicle Models																												
1. Initiated	25	9	63	A																								
2. Completed	1	4	64															▲										
PHASE III, TESTING																												
A. Lark Material Test (Asusa)																												
1. Initiated	1	9	63	A																								
2. Completed	28	2	64															▲										
B. 12K TVC Test (Asusa)																												
1. Initiated	1	9	63	A																								
2. Completed	28	2	64															▲										
C. Titan Size Nozzles (4 AEDC)																												
1. Initiated	1	1	64																									
2. Completed	31	3	64															▲										
D. Wind Tunnel Flight Simulation Checkout Tests (Asusa)																												
1. Initiated	1	12	63																									
2. Completed	28	2	64															▲										
E. Wind Tunnel Flight Simulation Model Tests (JPL)																												
1. Initiated	1	1	64																									
2. Completed	31	5	64															▲										

○ - PRESENT SCHEDULE DATE ▲ - ACCOMPLISHED
 □ - POTENTIAL CHANGE IN SCHEDULE ◊ - PREVIOUS SCHEDULE DATE

III. COMBUSTION INSTABILITY SCALING CONCEPTS

A. INTRODUCTION

1. Purpose

The combustion instability scaling program is an effort to predict analytically the longitudinal modes of instability of a subscale rocket engine; to determine from testing of this motor the longitudinal mode stability limits; to compare these results; and finally to utilize the results for determining the occurrence of transverse modes of instability for larger rocket engines. Appendix A, "Elements of Instability, Theory and Applications", has been provided in this report to assist in an understanding of the project objectives. It is a summary of material presented at the first quarterly progress review on 17 September 1963.

2. Approaches

This program is concerned with the stability of rocket engines as it is affected by chamber length, chamber pressure, and propellant mixture ratio. An empirical analysis will be attempted to determine the axial combustion distribution of this engine, which is required by the theoretical analysis.

For each test, a chamber pressure and a mixture ratio will be specified and held constant throughout the test. Once the thrust chamber has reached steady-state operating conditions, the chamber length will be increased during the test to study the stability effects resulting from the variation in chamber length. Two firings will be required for each operating point to keep the duration approximately 5.0 sec for each test. For the next test, the chamber

III, A, Combustion Instability Scaling Concepts (cont.)

pressure and/or the mixture ratio will be changed, the motor will be returned to its initial chamber length (a length-to-diameter ratio approximately equal to unity), and the test series continued.

B. PROGRESS DURING THE REPORT PERIOD

1. Thrust Chamber Assembly

a. Thrust Frame

The final design has been completed on the thrust frame and fabrication has begun. The frame has been designed with a safety factor of four and will be mounted to the test stand without any major test stand modifications. The frame will be supported by a four-point suspension system. The first suspension will mount the forward end of the thrust frame to the test stand interfaces. The second and third suspensions will be support struts from the test stand interface to the central portion of the thrust frame to prevent lateral motion during testing. The fourth suspension will be a cradle-type apparatus mounted between the bottom of the thrust frame and the deck of the test stand to help support the 1,000-lb weight of the thrust frame. The cradle will be swivel-mounted to the thrust frame to permit axial freedom of movement.

b. Combustion Chamber

The combustion chamber has undergone considerable design modification since the last report. The revised configuration, which is shown in Figure III-1, is divided into three sections. The first section is a 42.5-inch long, uncooled cylindrical section with a 6-inch inside diameter and an 8-inch outside diameter. The second section is an 18-inch long, water-cooled

III, B, Progress During The Report Period (cont.)

tube bundle in a cylindrical configuration with the longitudinal axis of the tubes parallel to the longitudinal axis of the motor. The third section provides support for the "Aerofoil."

The modification of the preliminary combustion chamber design was dictated by the results of the heat transfer and stress analyses. It was found that the material to be used for the cylindrical combustion chamber, Inconel 718, would yield under the combined hoop and thermal stress.

The new design of the chamber alleviates the sealing problem by placing the hot-gas seal 41 inches upstream of the injector face. The combustion zone is contained within the tube bundle and the third section. By fitting the injector with a cylindrical 38-inch extension, which fits inside the first section of the chamber, sealing surfaces are provided by the inside bearing surface of the chamber and the outside bearing surface of the injector extension. Aft of the hot-gas seal are five metallic seal rings spaced at five-inch intervals. These rings are used primarily for alignment of the chamber and the injector extension and secondarily for intermediate hot-gas seals. The consequence of this design is that the bearing surfaces used for sealing are never directly exposed to the combustion gases, thereby minimizing the amount of warping of the bearing surfaces. Any one of the three sections can be replaced with a minimum of time. A small amount of gaseous nitrogen will be injected into the cavity between the bearing surfaces during the countdown to prevent explosive gases from entering the cavity during the start sequence.

III, B, Progress During The Report Period (cont.)

The furnace-brazed tube bundle consists of 64 stainless steel tubes. A removable cylindrical shell of aluminum will encase the tube bundle. Cooling will be with water supplied to the tubes at 1000 psi and 15 gal/sec.

c. Injector

The propellant velocity in the injector feed channels has been decreased from 60 fps (the design velocity of the Titan II, second stage injector) to 20 fps in order to improve the fluid dynamics of the feed system. All other design considerations (e.g., the injector size, pattern, etc.) have remained unchanged. The final design of the injector is nearing completion and fabrication has begun ahead of schedule.

d. Nozzle

The nozzle used on this thrust chamber contains nine exhaust orifices rather than the customary single port. As a result, the length of the convergent section is only 3/8-inch. This short nozzle length is one method of building the required instability into the chamber. Two pieces make up the nozzle plate. The forward section, fabricated from ATJ graphite, provides not only the convergent section of the orifices and a short length of the divergent nozzle, but also a heat barrier for the aft section from the exhaust gases. The aft section of the nozzle is fabricated of 347 stainless steel to provide structural support for the graphite. Since erosion of the throat and thermal shock damage is expected during testing, the 1/2-inch thick graphite section will be replaced after every test.

III, B, Progress During The Report Period (cont.)

e. Aerofoil

The "Aerofoil" has been incorporated into the test series as a pitot tube to determine the mean, diametrical velocity profile of the combustion gases. Six total pressure ports and six static pressure ports are provided for the velocity measurements. Seven chromel-alumel thermocouples are also embedded within the "Aerofoil" material to obtain combustion temperature data.

2. Test Considerations

a. Test Schedule

The test schedule is in four parts:

- (1) Installation of the thrust chamber assembly in the test stand.
- (2) Checkout tests and four combustion distribution tests.
- (3) Combustion instability limits tests.
- (4) Repeat of tests yielding questionable data.

Figure III-2 indicates the conditions and objectives for each test. The assembly will be removed from the stand for a complete check during the data analyses which will be made both before and after the instability limits tests.

The fourth test in the scheduled series is a 10-second run to determine whether the test hardware is capable of withstanding the extended duration while the chamber is lengthened continuously from 6 inches to 22 inches. If the hardware can survive this environment, the schedule for instability limit

III, B, Progress During The Report Period (cont.)

testing will be changed from its present form (i.e., two 5-second tests at the same mixture ratio and chamber pressure but varying the chamber length on the first test from 6 to 12 inches and on the second test from 16 to 22 inches) to one 10-second test for each mixture ratio and chamber pressure.

Fewer tests of longer duration in this portion of the testing will permit additional testing at various mixture ratios and chamber pressures which can serve to better define the instability limits.

b. Instrumentation and Controls

The proper measurement of the steady-state and oscillatory chamber pressures is most important for this project. Two high frequency transducers will be used at the boundaries of the motor to measure the oscillatory variations of chamber pressure. A "small passage" transducer system utilizing a helium-cooled Kistler transducer will be mounted in the exact center of the injector face. At the approximate exit plane of the chamber, a special water-cooled Dynisco transducer will measure the pressure variations. The Dynisco transducer has been furnished to this project by Princeton University and is "special" in that the diaphragm is made of chrome-plated nickel to resist the high heat fluxes generated in the chamber during instability. It is estimated that this transducer modification will permit the survival of the transducer during heat fluxes as high as $25 \text{ Btu/in.}^2\text{-sec.}$

Seven Taber transducers are used to measure the steady-state combustion chamber pressures. One is located slightly off-center in the injector face beside the Kistler. The other six are placed at one-inch intervals,

III, B, Progress During The Report Period (cont.)

parallel to the chamber axis, upstream from the chamber exit so that the final six inches of the combustion chamber has one Taber per inch plus the high frequency transducer at the exit plane.

Figure III-3 presents the combustion chamber elongation system and the required hydraulic and electrical controls. The procedure for chamber elongation requires pressurizing the vent side of the actuation cylinders prior to test. Mechanical stops will be furnished so that the minimum length can be achieved without the exhaust nozzle being forced into the injector face during the pressurization of the cylinders. When the test is begun, the force of the chamber pressure will tend to elongate the chamber, but the pressure within the cylinders will exert a slightly greater retarding force. When the timer opens the actuator vent valve, the resultant force in the chamber will lengthen it at a rate that is controlled by the orifice in the vent system.

C. NEXT REPORT PERIOD

The final design of the combustion chamber will be completed and fabrication begun. The remaining hardware will continue through the fabrication cycle. Test stand systems modification will have begun. The theoretical instability zone investigations will be completed.

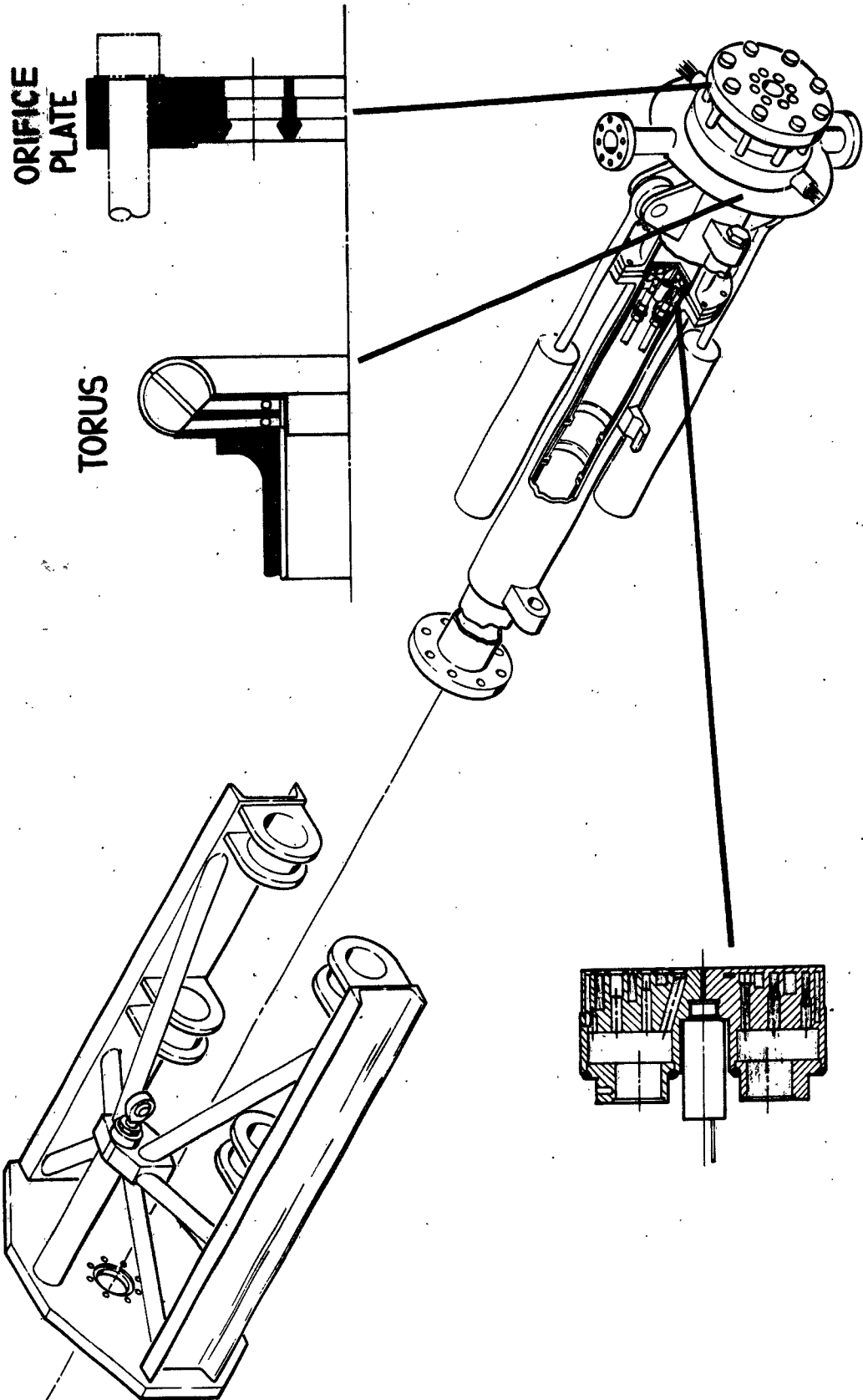
The milestone chart for this project is shown in Table III-1.

TABLE III-1

COMBUSTION INSTABILITY SCALING CONCEPTS MILEPOST CHART

COMBUSTION INSTABILITY SCALING CONCEPTS	PRESENT SCHEDULE			P R I O R	CY 63					CY 64					
	DAY	MO	YR		J	J	A	S	O	N	D	J	F	M	A
PHASE I, ENGINEERING DESIGN															
A. Concept Completed				A											
B. Predesign															
1. Initiated	1	7	63		A										
2. Completed	31	8	63				A								
C. Final Design Initiated															
1. Mount Completed	12	8	63			A	◊								
2. Thrust Chamber Completed	11	10	63				◊	▲							
3. Injector Completed	4	10	63					▲							
4. Actuation System Completed	12	8	63			A									
5. "Aerofoil"	11	10	63					▲							
PHASE II, FABRICATION INITIATED															
1. Mount Completed	4	11	63					▲							
2. Thrust Chamber Completed	6	12	63						▲						
3. Injector Completed	6	12	63						P	▲					
4. Actuation System Completed	16	12	63							▲					
5. Calibration Completed	24	12	63							▲					
PHASE III, TESTING INITIATED															
1. Test Stand Build-up Completed	6	1	64							▲					
2. Calibration Firings Completed	13	1	64							▲					
3. Test Program Completed	31	1	64							▲					
PHASE IV, ANALYSIS INITIATED															
1. Calculation of Theoretical Instability Zones Completed	15	12	63							▲					
2. Completion of Comparison Between Theoretical Zones and Test Results	22	4	64											▲	

◊ - PRESENT SCHEDULE DATE A - ACCOMPLISHED
 P - POTENTIAL CHANGE IN SCHEDULE ◊ - PREVIOUS SCHEDULE DATE



Variable Length TCA

Figure III-1

TEST N°	CHAMBER PRESS.(PSIA)	MIXTURE RATIO	DURATION (SEC)	REMARKS
1	500	1.60	3	BALANCE TEST SYSTEM CHECKOUT TEST AEROFOIL CHECKOUT TEST HARDWARE DURABILITY TEST
2		1.87	5	
3		2.10	5	
4	850	1.87	10	COMBUSTION DISTRIBUTION TEST
5		1.60	5	
6		2.10	5	
7		1.87	10	INSTABILITY LIMITS TEST
8	500	1.60	5	
9		1.60		
10		1.87		
11		1.87		
12		2.10		
13		2.10		
14	850	1.87		
15		1.87		

Figure III-2

Preliminary Test Schedule

HYDRAULIC-ELECTRIC
SYSTEM FOR
COMBUSTION CHAMBER ELONGATION

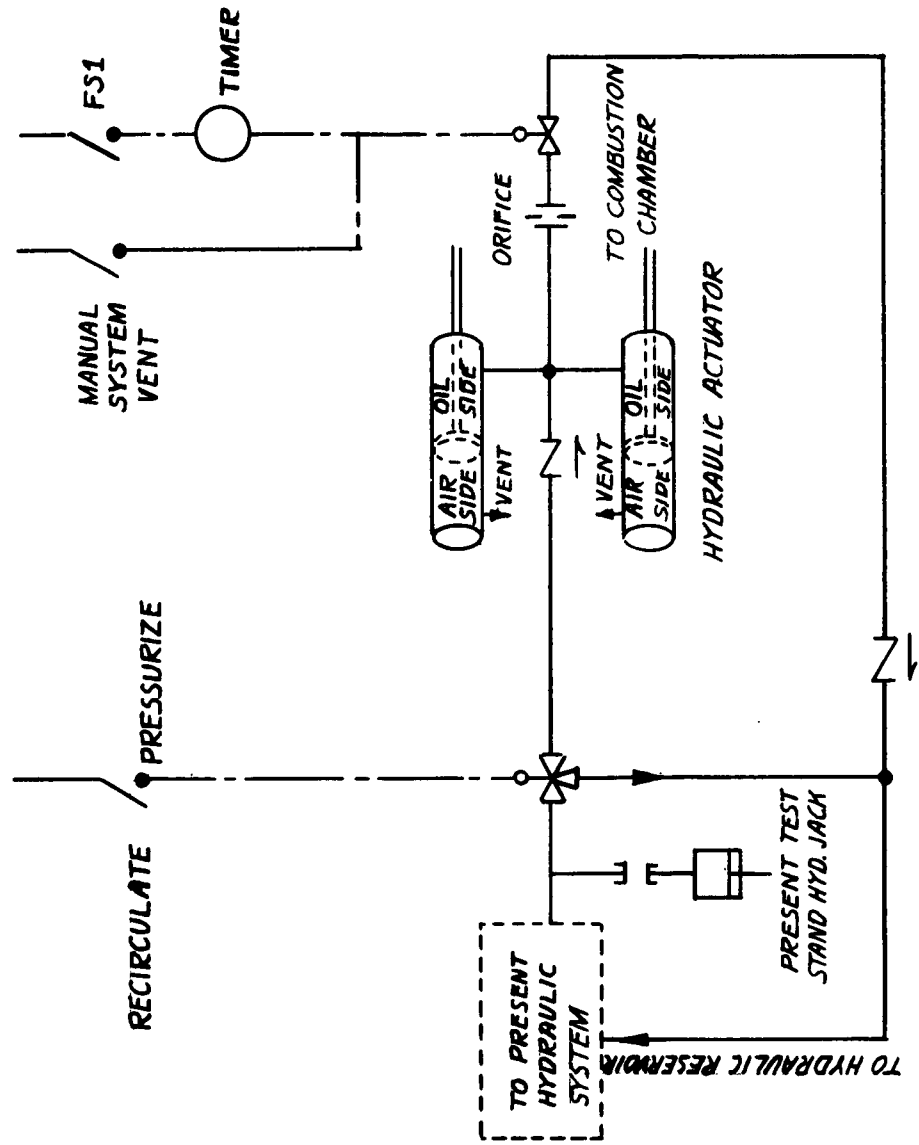


Figure III-3

Hydraulic - Electric System for Combustion Chamber Elongation

APPENDIX III-A

ELEMENTS OF INSTABILITY THEORY AND APPLICATIONS

APPENDIX III-A

TABLE OF CONTENTS

	<u>Page No.</u>
I. Instability Definition	III-A-1
II. Mechanisms of Instability	III-A-4
III. Instability Theory	III-A-4
IV. Application of the Time Lag Theory	III-A-7
A. Scaling Considerations	III-A-7
B. Design of the Subscale Chamber	III-A-7
V. Goals for the Project	III-A-9

FIGURE LIST

	<u>Figure No.</u>
Combustion Instability - Definition	III-A-1
Combustion Instability - Classification	III-A-2
High Frequency Instability - Classification	III-A-3
Combustion Instability - Mechanisms	III-A-4
Sensitive Time Lag Theory	III-A-5
High Frequency Instability Zones	III-A-6
Determination of Operating Region	III-A-7

I. INSTABILITY DEFINITION

Figure III-A-1 represents a rocket thrust chamber that has successfully started, has operated at steady state for a time interval, and suddenly has become unstable. The stable and unstable sections of the test are amplified and indicate the chamber pressure characteristics during each of the operating conditions.

Normal, stable operation of a thrust chamber is characterized by "rough" combustion where there appears to be no wave or phase relationship to the resultant chamber pressure fluctuations. This roughness can never be eliminated from a liquid rocket inasmuch as it is inherent to the turbulent, heterogeneous combustion process occurring within the chamber. However, when the operation becomes unstable, the chamber pressure takes on a very definite wave shape as the oscillations become extremely organized. It is not unusual for a motor to begin a test stably and then, for some unknown reason, suddenly become unstable. The cause of this undesirable transition is that the "rough" combustion noise, consisting of many acoustic frequencies and accounting for the very irregular wave shape, has matched one of the natural resonant frequencies of the combustion chamber. Therefore, instability can be thought of as an undesirable agreement between the combustion process and the combustion chamber to a preferred frequency.

A salvation to the rocket industry is that the combustion process and chamber are not always in agreement with a preferred frequency. Therefore, in order to have stable operation in rocket engines, disagreement must be built into the engine. For the present project, in order to study instability, the reverse approach is applied. That is to say, the thrust chamber assembly was purposely

I, Instability Definition (cont.)

designed to be unstable so that the exact limits of the instability zone can be determined. Once this instability zone is known, it becomes a relatively easy matter to design a subscale thrust chamber that operates in a region where the probability of detrimental instability has been reduced. Once this region has been established, the large rocket engine can be designed by scaling the smaller model to the larger dimensions. If the design of future rocket engines incorporates these subscale considerations (i.e., a compromise between the desired performance and instability) many future programs will not experience some of the difficulties that are present in current programs.

Three major types of instability frequencies must be considered.

Figure III-A-2 illustrates the two most common types: low frequency and high frequency. The third type of instability, intermediate frequency, has not been detected as often as the first two types.

The classification of low frequency instability is assigned to pressure oscillations whose wave lengths are long compared to the chamber length. Low frequency instability is commonly termed "chugging" because pressure oscillations are slow enough to couple themselves with the feed system and result in propellant flow variations as the propellants enter the combustion chamber. Because of the long wave lengths, the pressure at all points within the chamber will be approximately the same, as indicated by Figure III-A-2.

To pressure oscillations with wave lengths approximately twice the chamber length or diameter, the classification of high frequency instability is assigned. The definition of instability presented at the beginning of this report described

I, Instability Definition (cont.)

high frequency instability. These frequencies of instability are of an acoustical nature since the combustion chamber must become unstable at one of its natural harmonic frequencies.

While "chugging" is fairly well understood and a rocket engine feed system can be designed to eliminate "chugging", high frequency instability is much more deceptive in that there is more than one mode of instability. High frequency instability, commonly referred to as "screaming," has three modes of instability as shown in Figure III-A-3.

The longitudinal mode of "screaming" can be described as a plane wave that travels the longitudinal axis of the chamber. The longitudinal mode is not a singular phenomenon but is a family. That is to say, a chamber might become unstable in the first longitudinal mode, or the second, or the third, or any higher mode of that family. The longitudinal modes of instability are generally the least destructive type of instability.

Figure III-A-3 illustrates an additional complexity of "screaming," in that along with the longitudinal family, there exist two other families: radial and tangential. The latter two families are capable of existing by themselves or in combinations. These two families comprise the transverse modes of instability.

To make matters worse, the longitudinal family and the transverse family can combine and exist together. If they combine, a chamber will be unstable longitudinally, radially, and tangentially simultaneously which constitutes a

I, Instability Definition (cont.)

complex chamber pressure oscillation and an almost insurmountable problem in deciphering which mode of instability is present.

II. MECHANISMS OF INSTABILITY

Figure III-A-4 is a block diagram which illustrates the mechanisms of instability for both "chugging" and "screaming."

The tank pressure, P_T , forces the propellant through the flow circuit and through the injector, the flow process system. The propellants are injected at a flow rate, W_i , into the chamber where combustion and fluid dynamics create chamber pressure, P_c .

For "chugging," the P_c must oscillate slowly enough to affect the flow process system as indicated by the middle circuit. The structure circuit below it can also affect the combustion process, if the structure is subject to vibration while the engine is running. Both circuits affect the flow rate of propellants into the chamber.

"Screaming," on the other hand, is not dependent on the variance of injection flow rates. Because of its high frequencies, the requirement for this mode is an acoustical coupling in the combustion chamber, i.e., the previously mentioned agreement between the combustion process and the combustion chamber.

III. INSTABILITY THEORY

Before discussing the theory used for this project, it must be mentioned that there are numerous instability theories being developed at present. Various authors have approached the topic of instability from aspects such as available

III, Instability Theory (cont.)

energy, vaporization mechanisms, chemical mechanisms, burning rates, detonations, and dimensional analysis. However, the majority of these approaches are not yet sufficiently developed to be used as a working tool. Many still need to be completely formulated and "proven" experimentally. Some are only one dimensional cases, with years of work ahead before completion of the three dimensional models. Many of these theories hold much promise when they are fully developed and experimentally verified.

The theory used in this instability investigation, the combustion sensitive time lag theory developed by L. Crocco and his associates at Princeton University, is a workable, three dimensional model that has been experimentally verified for both longitudinal modes and transverse modes of instability. To many purists, the theory may make too many simplifying assumptions; however, within the frame of reference that the theory was developed, it still represents a good "tool" for instability investigations.

Figure III-A-5 indicates the basic components of the combustion sensitive time lag theory. The theory is concerned with two parameters: the pressure index of interaction between the combustion processes and the oscillations in the combustion chamber, n , and the sensitive part of the total time lag, τ .

When the liquids in a bipropellant rocket are injected into the chamber, there is a short time delay before the liquids are converted into exhaust gases by combustion. This time delay, or time lag, represents many processes that must occur from the instant the liquid leaves the injector to the instant of complete combustion. There is some time delay for the liquid to enter the

III, Instability Theory (cont.)

chamber, a delay for the liquid to separate into droplets, a time delay for mixing, a time delay for the initial vaporization of the droplet to begin, and more delays until, finally, the droplet is gone and combustion gases only remain.

Assume that a motor is operating stably and then, for some unknown reason, a pressure oscillation occurs. Some of the mentioned time delays will be affected by this pressure perturbation (e.g., vaporization) and some time delays will not be affected (e.g., atomization). Therefore, the total time lag is the summation of two parts: an insensitive part and a sensitive part.

The "interaction index", n , is a measure of the sensitivity to pressure disturbances.

With these two parameters, the time lag theory states that given an injector pattern, propellant combination and operating condition, a specific (n, γ) point will result. If the point falls into the middle region, the chamber will be unstable. If the point falls outside the middle region, the chamber will be stable. If the point falls outside the envelope, it might be stable and then become unstable if disturbed (e.g., by a gun pulse).

The theory will analytically provide the zones of instability by considering the acoustics of the thrust chamber assembly. Only actual testing will provide the (n, γ) value which is a function of injector pattern, propellant properties, and operating conditions. Actually, testing will provide not one point for (n, γ) but an operating region because of experimental uncertainties.

III, Instability Theory (cont.)

Once the operating region has been established by testing and by using the analytical results of the theory, every possible mode of instability can be forecast. It is at this time that suggestions can be made which will move the instability zones away from the operating zone with the result that the engine will generally be more stable. The present program is concerned with the demonstration of this procedure by determining an (n, γ) region for the second-stage Titan II engine and comparing the results with actual full-scale test experience.

IV. APPLICATION OF THE TIME LAG THEORY

A. SCALING CONSIDERATIONS

Three principles were used in scaling the subscale model to the thrust chamber assembly of Titan II second stage.

1. The ratio of the combustion chamber area to the total throat area was kept consistent with the Titan II thrust chamber assembly.
2. The attenuation of the instability frequencies of the subscale chamber was decreased by 90%.
3. The injection density of the two chambers was kept the same.

B. DESIGN OF THE SUBSCALE CHAMBER

As pointed out above, the possibility exists for longitudinal modes of instability to combine with the transverse modes resulting in a chamber with complicated instability characteristics. Since it is preferred not to design a chamber that has all three types of instability present, several considerations can be given to eliminate the transverse modes from the instability picture which allows study of only longitudinal modes.

IV, B, Design of the Subscale Chamber

Figure III-A-6 is a composite illustration which indicates the method of decreasing the probability of experiencing transverse modes that was used in the design of the chamber. As the chamber diameter is decreased, the sensitive time lag for a minimum value of n of the first tangential mode continually decreases (shifts left) while the minimum value of n continues to increase. Consequently, by choosing a sufficiently small diameter, the tangential instability zones will have been "shifted" away from the thrust chamber's operating zone. The subscale chamber has a 6-inch chamber diameter which is felt to be sufficient for eliminating the transverse modes from this test series.

Figure III-A-6 also indicates the variance of the unstable (n, γ) zones as the chamber length is increased. When this family of lines is presented for a standard exhaust nozzle and a short exhaust nozzle, as it is presented in Figure III-A-7, and the anticipated operating zone is superimposed onto the figure, it is immediately obvious how the subscale chamber will determine the exact location of the operating zone.

The exhaust nozzle used on the chamber is another instability feature. The flat exhaust nozzle with the short orifices provides a better defined acoustic wall, whereas the conventional, one-element exhaust nozzle with its relatively long convergent section attenuates the frequencies due to the inability of the nozzle to provide a reflecting surface with a minimum amount of acoustic scattering.

V. GOALS FOR THE PROJECT

1. Create instability in the longitudinal modes only.
2. Accurately define the operating (n, γ) zone.
3. With the definition of the operating zone, successfully predict the transverse modes of instability for the parent full-scale rocket engine.

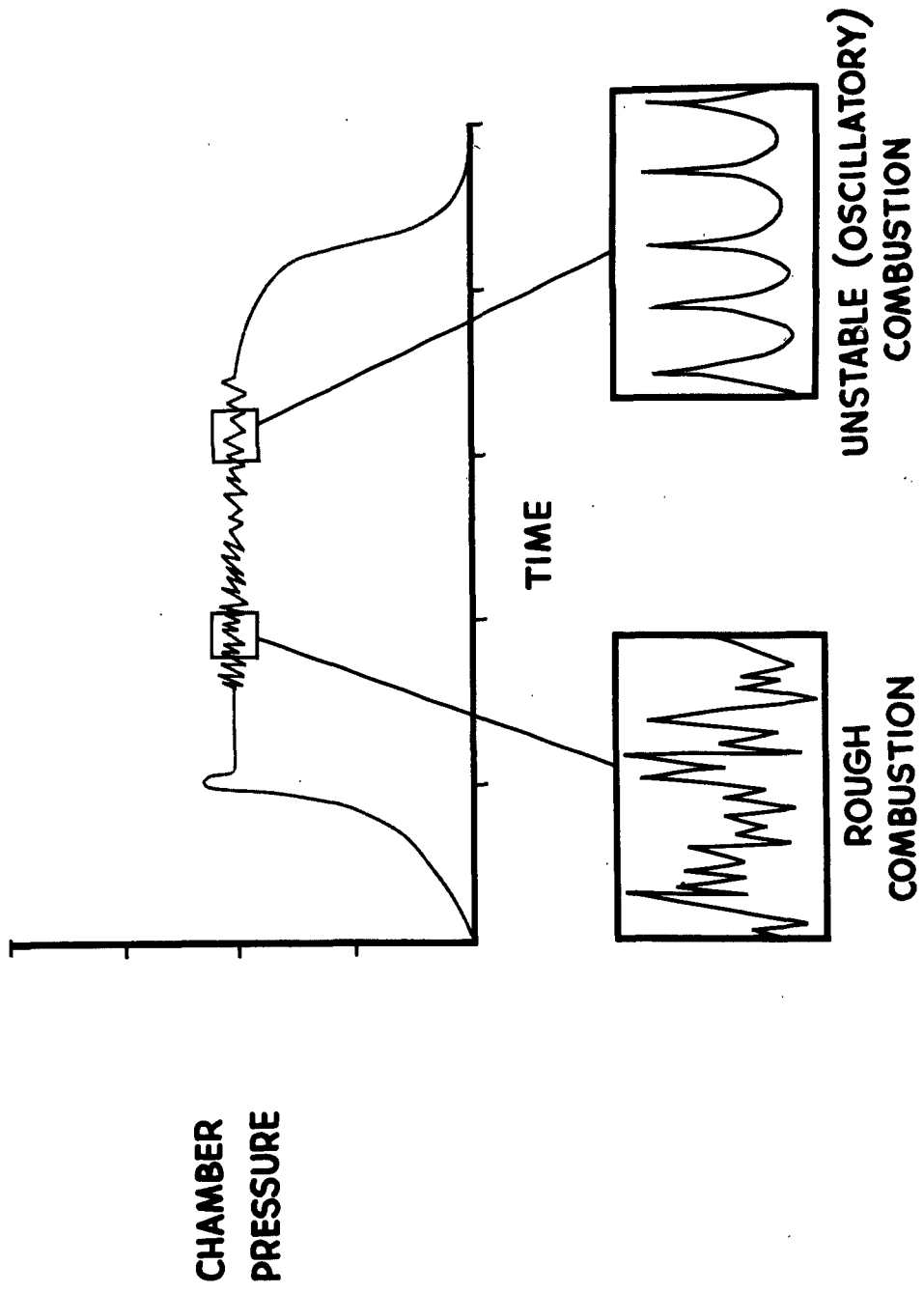
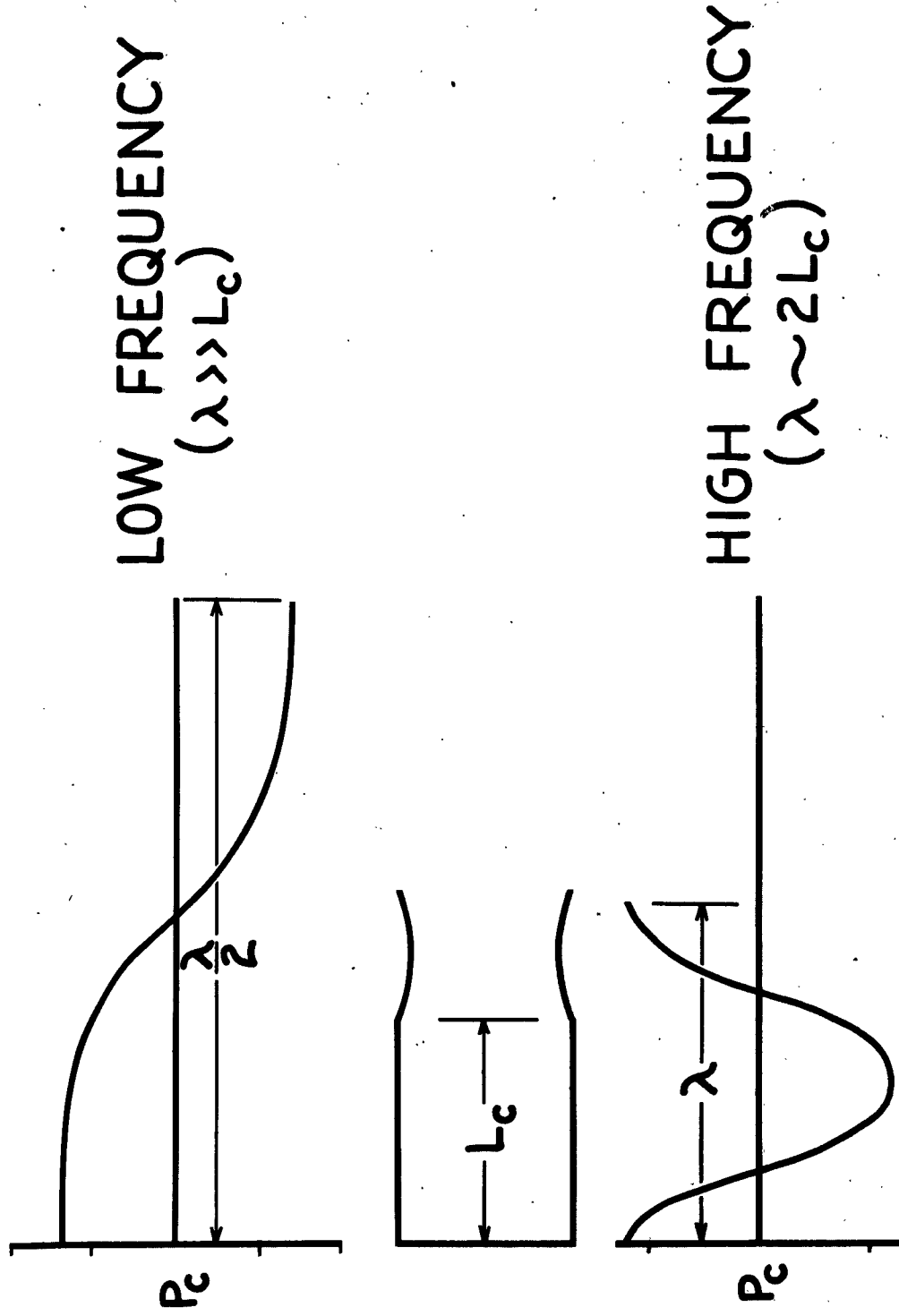


Figure III-A-1



Combustion Instability - Classification

Figure III-A-2

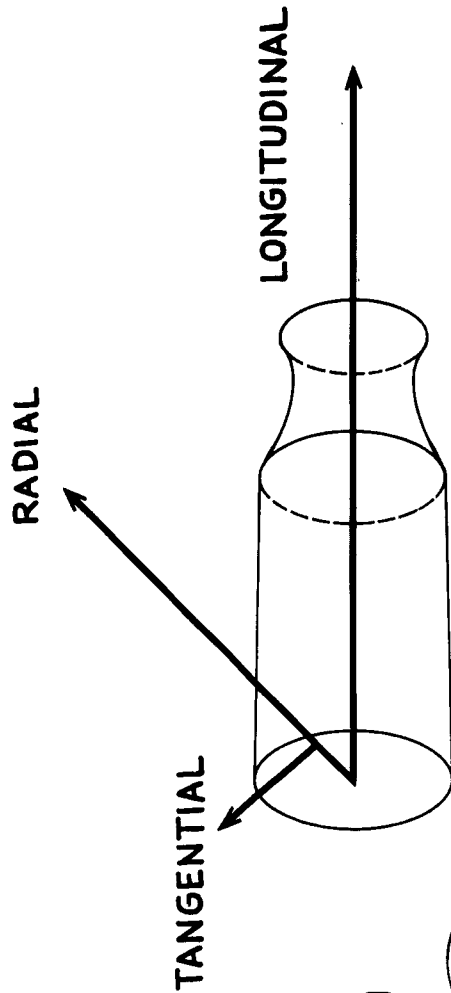
HIGH FREQUENCY INSTABILITY - CLASSIFICATION

LONGITUDINAL

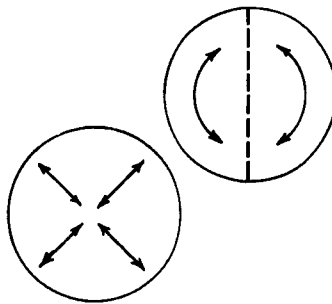
- FIRST $f \approx C/2L$
- SECOND $f \approx C/L$

TRANSVERSE

- RADIAL
- TANGENTIAL
(1) STANDING
(2) SPINNING
- COMBINED
RADIAL - TANGENTIAL
(1) STANDING
(2) SPINNING



CYLINDRICAL COORDINATES



COMBINED

- LONGITUDINAL - TRANSVERSE

Figure III-A-3

COMBUSTION INSTABILITY - MECHANISMS

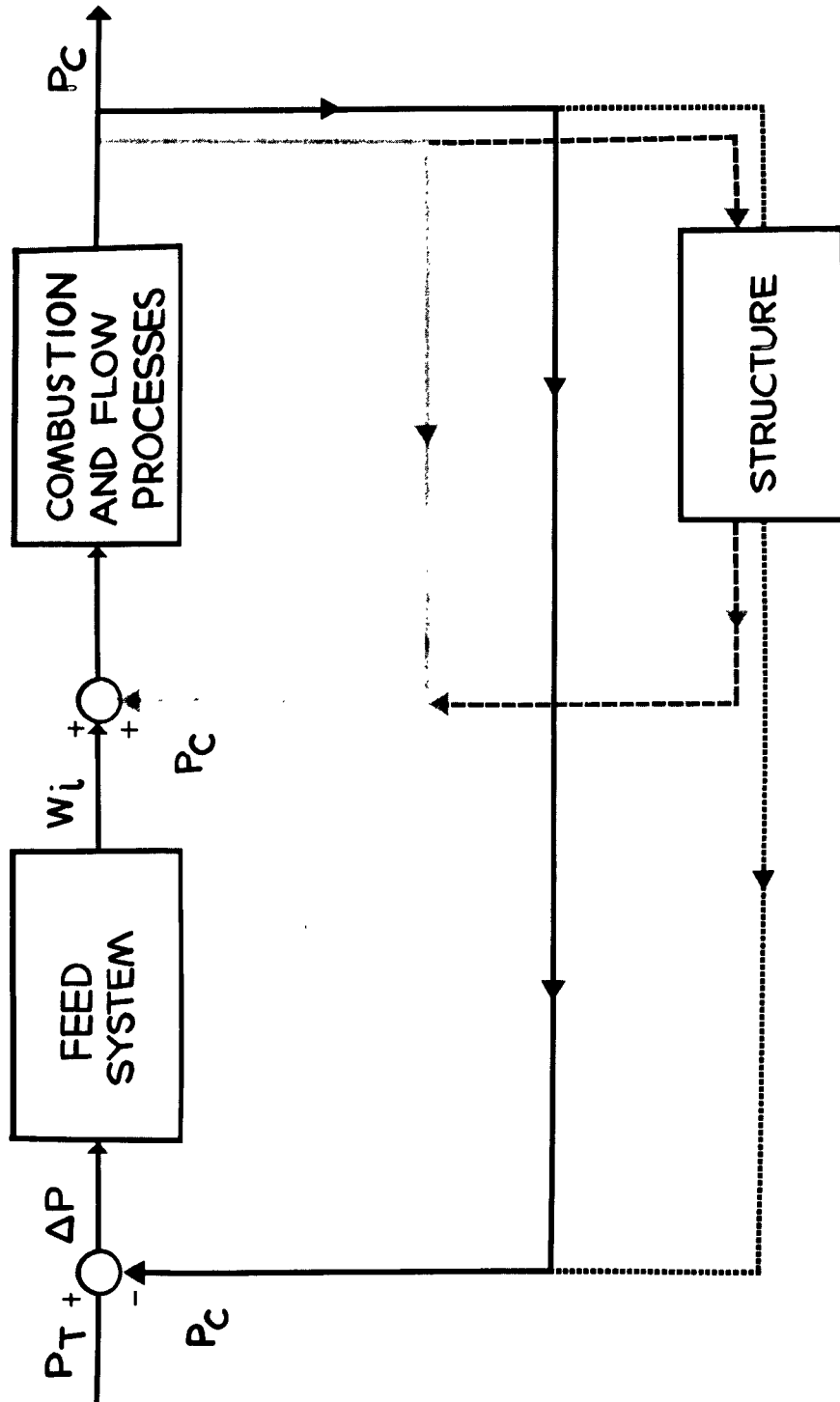


Figure III-A-4

SENSITIVE TIME LAG THEORY

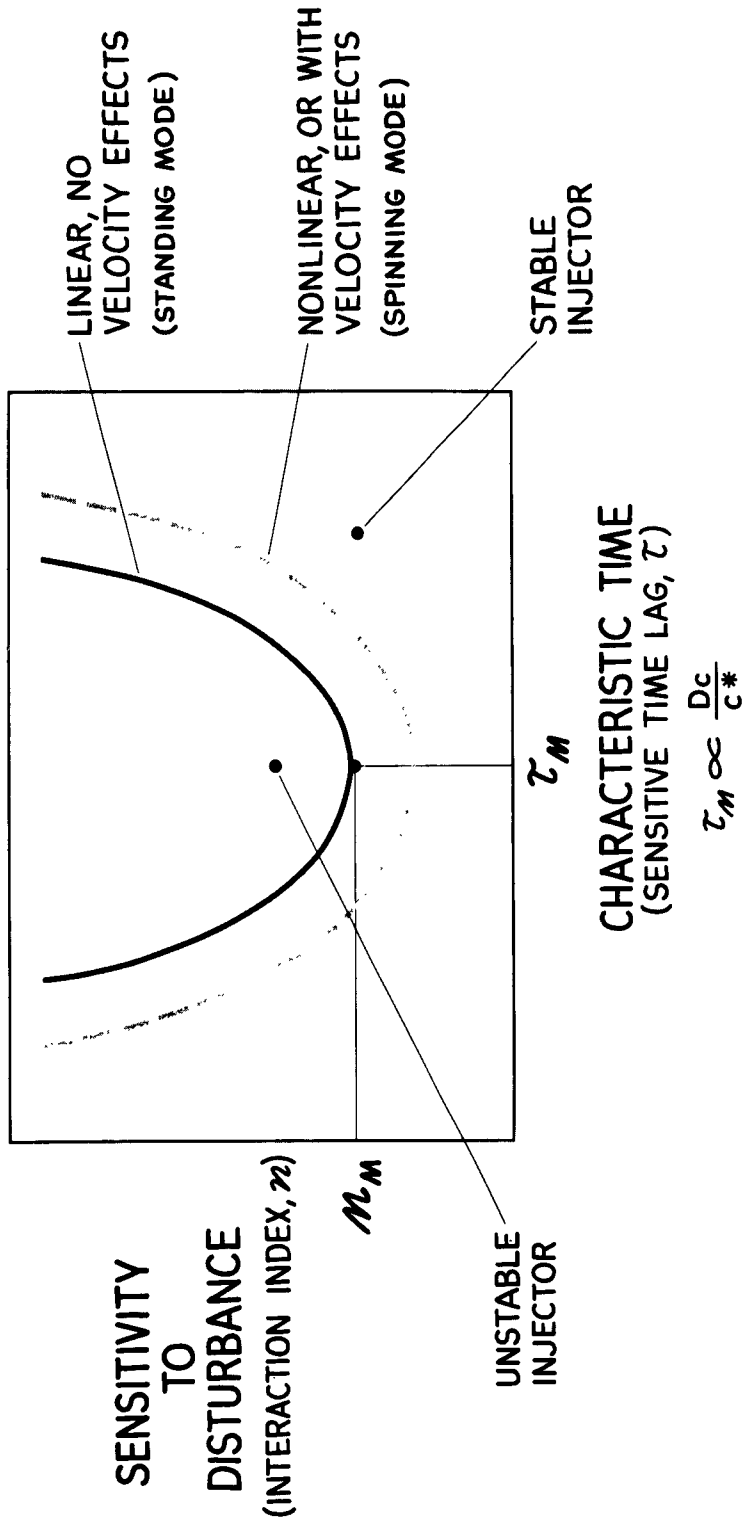
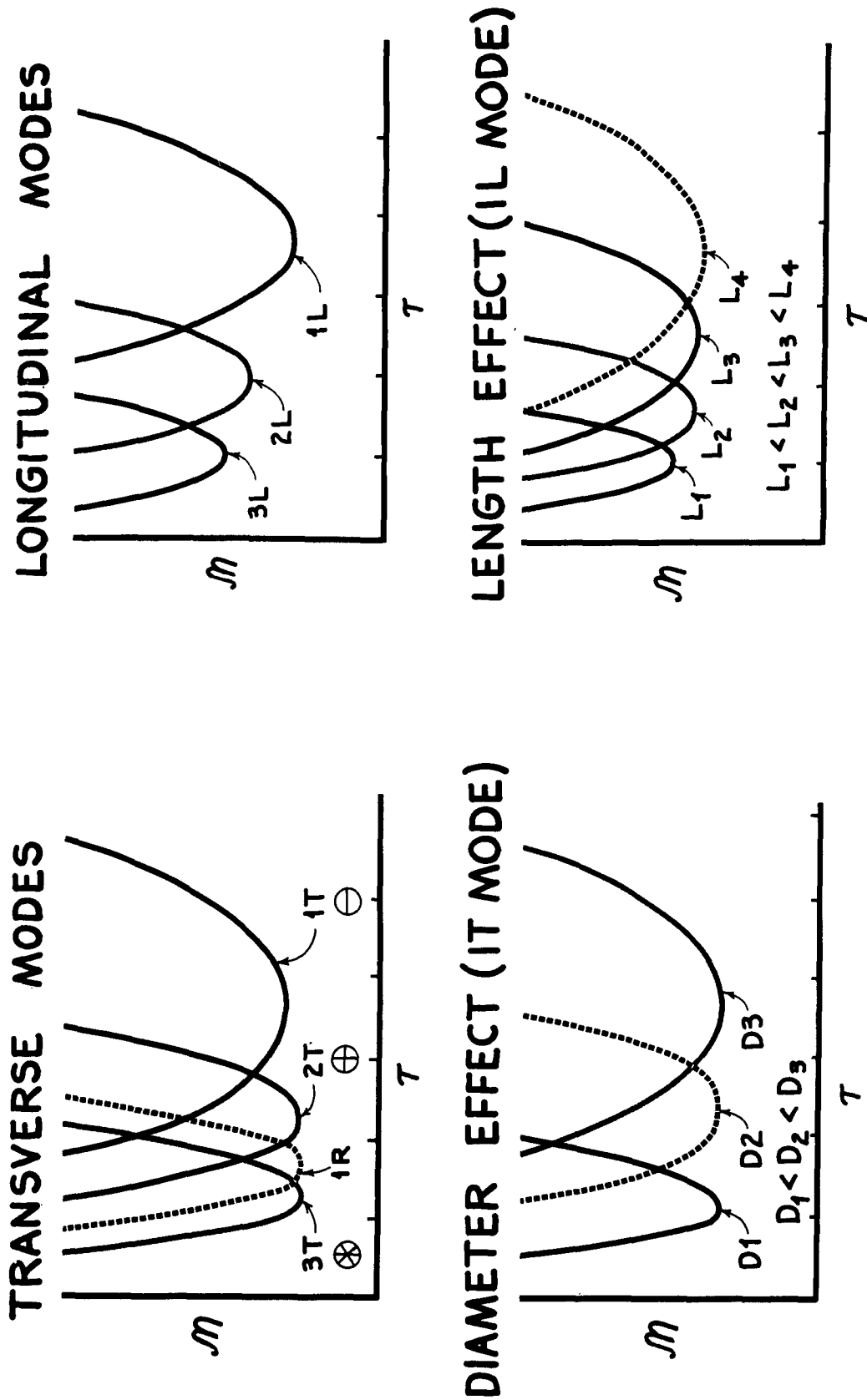


Figure III-A-5

HIGH FREQUENCY INSTABILITY ZONES



High Frequency Instability Zones

Figure III-A-6

SUBSCALE TCA TESTING

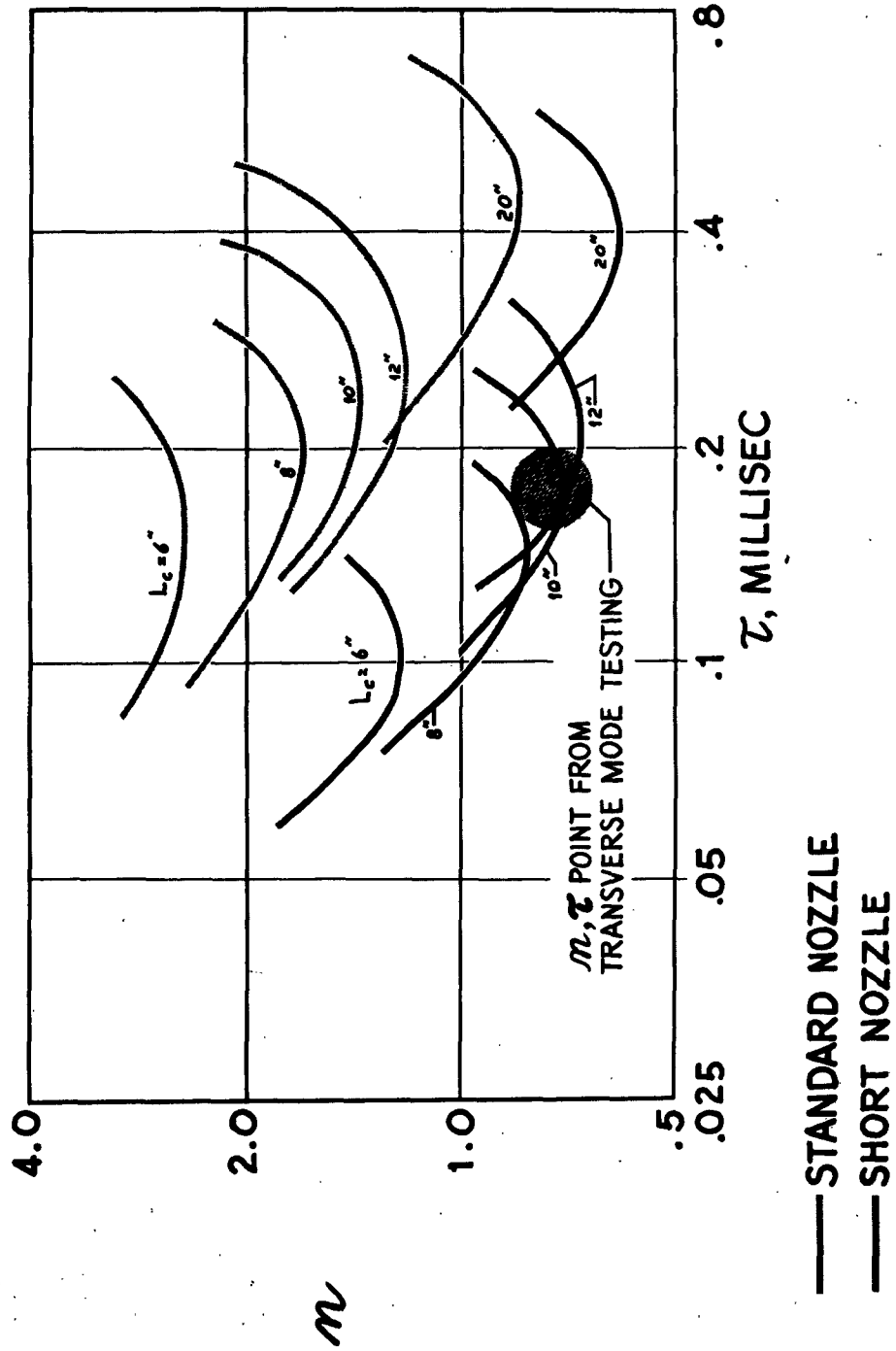


Figure III-A-7

Determination of Operating Region

IV. ABLATIVE THRUST CHAMBER

A. INTRODUCTION

1. Purpose

The purpose of this project is to demonstrate the feasibility of large ablatively-cooled thrust chambers for high performance, liquid rocket engines operating at chamber pressures up to 300 psia for extended durations. The ablative chambers will embody the compression-molded building block concept.

2. Approaches

Six thrust chambers fabricated under Contract AF 04(647)-652/SA33 will be used with injectors developed on the Apollo Service Module Engine Program (Contract NAS 9-150). A water-cooled transition will be used to adapt the Apollo injector to the ablative chambers which have a Titan II second-stage configuration. The thrust chambers are described in detail in the final report for Contract AF 04(647)-652/SA33⁽¹⁾, and are briefly described in Report 212/SA 3-2.2-M-1 of the current series of monthly progress reports.

B. PROGRESS DURING THE REPORT PERIOD

1. Transition Section

The analysis and design of the water-cooled transition section was previously completed, and fabrication was initiated during this report period. Present shop load indicates the transition section will be completed on schedule.

2. Injector

The selection of an Apollo injector has been reviewed with the Apollo Program Manager on the basis of performance availability. Avail-

(1) BSD-TDR-63-118, "Ablative Thrust Chamber Feasibility," 28 June 1963.

IV, B, Progress During The Report Period (cont.)

ability of the stable aluminum injectors has become very limited because of the Apollo test requirements which include a 2100-sec total firing duration on each injector. However, two of the earlier stainless-steel Apollo injectors (modified from Titan 91-5 injectors) will be available. One of these (S/N AT-6) has been fired 15 times and found to be stable, except when pulsed with a 10-grain explosive charge. This injector for the early Apollo program utilized a triplet pattern. As back up injectors there are two possible choices: Apollo injector AT-3, similar in design to AT-6, but which proved to be unstable in testing; and FP-1, an aluminum, cooled-baffle injector for which only a few seconds firing have been accumulated. Before injector AT-3 would be used, the orifices would be plugged and redrilled to the current Apollo pattern. The use of injector FP-1 as back up is more desirable, but this is dependent on a decision as to its availability from the Apollo program.

3. Ablative Chambers

Fabrication of the fifth steel shell is complete and the ablative components are installed. Final interior contouring is the only major operation remaining on this chamber. Fabrication of the sixth steel shell is complete except for stress relieving, after which the ablative components will be installed.

4. Selection of Firing Parameters

The proposed firing parameters were reported at the Quarterly Program Review. A request for formal approval of the parameters will be submitted by letter to the program monitor at the Rocket Propulsion Laboratory.

C. NEXT REPORT PERIOD

Fabrication of six chambers will be completed and they will be placed in storage pending firing. Fabrication of the transition section should also be essentially completed. Apollo injector AT-6 will be secured and examined for condition. Coordination will continue with Apollo Program personnel regarding the availability of injector FP-1. Heat transfer and stress analysis will be initiated on the selected injectors to ensure compatibility with the more severe environment of the planned tests.

The program schedule is presented in Table IV-1.

Table IV-1

Ablative Thrust Chambers Feasibility Milepost Chart

ABLATIVE THRUST CHAMBER FEASIBILITY	PRESENT SCHEDULE			P R I O R	Calendar Year 1963												Calendar Year 1964				
	DAY	MO	YR		J	J	A	S	O	N	D	J	F	M	A	M					
Phase I, TEST PREPARATION																					
A. Design of Ablative Chamber				A																	
B. Fabrication of Ablative Chamber																					
1. Chamber 284528-9				A																	
2. Chamber 278120-149	31	8	63					A													
3. Chamber 278120-259	21	8	63					A													
4. Chamber 278120-189	31	8	63					A													
5. Chamber 284528-29	15	10	63					◆	◆												
6. Chamber 278120-219	10	10	63					◆	◆												
C. Design of Metal Shell				A																	
D. Fabrication of Metal Shells (2)	4	10	63					◆	◆												
E. Design of Transition Section	10	8	63					A	◆												
1. Heat Transfer Analysis	10	7	63					A	◆												
F. Fabrication of Transition Section	30	10	63							◆											
G. Selection of Injectors	31	10	63					◆	◆												
H. Injector Fabrication (if required)	30	12	63						◆												
I. Uncooled Chamber Acquisition	15	6	63	A																	
J. Selection of Instrumentation	30	9	63						◆												
K. Selection of Firing Parameters	15	9	63					A	◆												
L. Ablative Chamber Assembly	31	12	63							◆											
M. Installation of Instrumentation	30	11	63							◆											
PHASE II, FIRING TESTS																					
A. Injector Checkout	30	11	63							◆											
B. Ablative Chamber Test	31	1	64													◆					
PHASE III, DATA EVALUATION																					
A. Data Reduction	21	2	64													◆					
B. Chamber Evaluation																					
1. Performance	16	3	64													◆					
2. Materials Evaluation	16	3	64													◆					
3. Comparison with Subscale Tests	15	4	64													◆					

◆ - PRESENT SCHEDULE DATE A - ACCOMPLISHED
 P - POTENTIAL CHANGE IN SCHEDULE ◇ - PREVIOUS SCHEDULE DATE

V. PROGRAM REPORTING

Listed in Table V-1 is the schedule for contract reports.

Report 212/SA3-2.2-M-3

DISTRIBUTION LIST

<u>External</u>	<u>No. of Copies</u>
Commander Ballistic Systems Division Air Force Systems Command Norton Air Force Base, California Attn: BSRPA	1
Commander Ballistic Systems Division Air Force Systems Command Norton Air Force Base, California Attn: BSRPT	1
Defense Document Center Arlington Hall Station Arlington, Virginia	10
Space Technology Laboratories Norton Air Force Base, California Attn: Mr. A. I. Hoffman	1
Commander Rocket Propulsion Laboratory Edwards, California Attn: DGREA	5
Liquid Propellant Information Agency Applied Physics Laboratory John Hopkins University 8621 Georgia Avenue Silver Springs, Maryland	2
<u>Internal</u>	47